In Vivo Serial Imaging of Regenerating Corneal Nerves after Surgical Transection in Transgenic Thy1-YFP mice

Abed Namavari, Shweta Chaudhary, Joy Sarkar, Lisette Yco, Kunal Patel, Kyu Yeon Han, Beatrice Y. Yue, Jin-Hong Chang, and Sandeep Jain

Purpose. To determine the effect of lamellar transection surgery on the nerve fiber density (NFD) and pattern of nerve regeneration in the cornea of *thy1*-YFP transgenic mice.

Methods. Wide-field stereo fluorescence microscopy was used to obtain serial images of nerves in live *thy1*-YFP mice, which express a fluorescent protein in their axons. NFD (mm/mm^2) was calculated from maximum intensity projection images as the total length of fibers within the area of the contour in which nerves were traced. Whole-mount confocal microscopy was performed to analyze the arrangement of nerves and the types of regenerating fibers.

Results. NFD in normal corneas was 35.3 ± 1.8 mm/mm^2. Stereo fluorescence microscopy revealed the presence of a subbasal hairpin nerve layer and an intrastromal nerve trunk layer. After surgery, regenerative sprouting was observed from transected distal ends of intrastromal nerve trunks. NFD also increased, with this increase being maximal between 4 and 6 weeks after surgery. NFD approximated baseline values at 6 weeks and did not change any further at 8 weeks. Regenerated nerves did not readopt the normal corneal nerve arrangement. A dense interlacing network of regenerated nerves was present in the corneal bed. Branches from this network traversed the flap to innervate the epithelium. Immunofluorescence staining revealed that regenerating fronds contained peptidergic nociceptive fibers (positive for calcitonin gene-related peptide and substance P) and myelinated non-nociceptive fibers (positive for neurofilament 200).

Conclusions. Although corneal NFD recovers to normal levels by 8 weeks after nerve transection, the arrangement of regenerated nerves is abnormal. (*Invest Ophthalmol Vis Sci.* 2011; 52:8025–8032) DOI:10.1167/iovs.11-8332

Sensory innervation to the cornea from the trigeminal ganglion is important for perceiving stimuli, maintaining hydration, and avoiding injury. Corneal nerve dysfunction forms the pathophysiologic basis of ocular diseases, causing considerable morbidity such as neurotrophic keratitis and dry eye disease.[1,2] Ophthalmic surgical procedures, including corneal transplant, radial keratotomy, photorefractive keratectomy, and laser-assisted in situ keratomileusis (LASIK), cause corneal nerve disruption and dysfunction.[3]

Corneal nerve imaging (e.g., optical coherence tomography and confocal laser scanning) has provided insight into the process of corneal reinnervation. Clinical studies have shown that corneal nerves regenerate over several years after surgical transection; however, the nerve density never returns to presurgery values. For example, subbasal nerve density decreased by 82% in 5 days after LASIK.[4] A gradual increase in density was observed at 2 weeks after surgery; however, even 2 years after LASIK, nerve density was only 64% of preoperative values.[4] Similarly, subbasal nerve density is not restored to normal even 40 years after penetrating keratoplasty.[5] Median subbasal nerve density in clear grafts is also significantly lower than that in normal corneas.[6] Although these studies have described the phenomenological process associated with corneal reinnervation, the associated molecular events remain largely unknown. As a result, despite the clinical need to promote corneal nerve regeneration in neurotrophic corneas, few specific therapeutic interventions are available.[7] One reason for insufficient progress in this area is the limited availability of methodologies to investigate the effect of interventions on corneal nerve regeneration. Fortunately, the relatively recent introduction of neurofluorescent *thy1*-YFP mice has made sequential in vivo investigations of corneal nerves feasible.[8]

Here, we performed serial in vivo imaging in *thy1*-YFP mice to analyze changes in nerve fiber density (NFD) and the pattern of regenerated nerves after lamellar transection surgery. NFD was defined as the total length of fibers within the area of the contour in which nerves were traced.[9] This study provides baseline data for future investigations of interventions to improve nerve regeneration.

Methods

Animals

All animal experiments were conducted according to the ARVO Statement for the Use of Animals in Ophthalmic and Vision Research. The animal protocol was approved by Animal Care Committee of the University of Illinois at Chicago. Neurofluorescent homozygous adult mice (6–8 weeks old) from the *thy1*-YFP line were purchased from Jackson Laboratories (Bar Harbor, ME). For in vivo experiments, mice were anesthetized with intraperitoneal injections of a combination of ketamine (20 mg/kg; Phoenix Scientific, St. Joseph, MO) and xylazine (6 mg/kg; Phoenix Scientific). For terminal experiments, mice were killed according to animal committee protocols. Animals were killed and excluded from the study at any point if they developed corneal neovascularization or opacity.

Animal Surgery

Surgery was performed on the left eye of each animal. The central cornea was marked with a 2-mm-diameter disposable trephine (Visipunch; Huot Instruments, Menomonee Falls, WI). A partial-thickness

From the Department of Ophthalmology and Visual Sciences, University of Illinois at Chicago, College of Medicine, Chicago, Illinois.

Supported by National Eye Institute Grant EY018874 (SJ) and Core Grant EY01792 and by Research to Prevent Blindness.

Submitted for publication August 1, 2011; revised August 26, 2011; accepted August 30, 2011.

Disclosure: **A. Namavari**, None; **S. Chaudhary**, None; **J. Sarkar**, None; **L. Yco**, None; **K. Patel**, None; **K.Y. Han**, None; **B.Y. Yue**, None; **J.-H. Chang**, None; **S. Jain**, None

Corresponding author: Sandeep Jain, Department of Ophthalmology and Visual Sciences, University of Illinois at Chicago, 1855 W. Taylor Street, Chicago, IL 60612; jains@uic.edu.

incision 0.2 mm in length was made perpendicularly to the corneal surface, tangential to the circular trephine mark, using a 15°, 5.0-mm standard angle knife (I-KNIFE model 8065401501; Alcon, Fort Worth, TX). The peripheral lip of the corneal incision was depressed to penetrate the stroma centripetally, thus creating a corneal pocket. A 1.0-mm paracentesis knife (Clearcut Sideport model 8065921540; Alcon) was used to expand the corneal pocket to the 2-mm-diameter trephine mark. Next, a 45°, 1.75-mm subretinal spatula (Grieshaber UltraSharp model 682.11; Alcon) was used to enter the corneal pocket, incise it from within (ab-interno), and exit at the 2-mm-diameter trephine mark. A Vannas scissor was used to extend the circumferential incision along the trephine mark. At three points (each approximately 0.5 clock hours), the corneal pocket was left unincised. This formed three hinges that allowed the flap to remain attached to the cornea in the absence of sutures. Animals received antibiotic ointment in the eye and underwent suture tarsorrhaphy, which was opened after 3 days.

Stereo Fluorescence Imaging

Six mice underwent sequential nerve imaging. Of these, one was excluded from the analysis because of corneal scarring. Sequential in vivo photography was performed using a fluorescence stereoscope (StereoLumar V.12; Carl Zeiss Meditec GmbH, Oberkochen, Germany) equipped with a digital camera (Axiocam MRm; Carl Zeiss Meditec GmbH) and image analysis software (AxioVision 4.0; Carl Zeiss Meditec GmbH). Images were acquired at baseline and at 2-week intervals for the duration of the study. An anesthetized *thy1*-YFP mouse was placed on the stereoscope stage. Seven microliters of proparacaine (0.5%; Bausch & Lomb, Tampa, FL) was then applied for 3 minutes, and the pupil was constricted with carbachol 0.01% (Miostat; Alcon) for 5 minutes. Z-stack images were obtained at 5-μm intervals and compacted into one maximum intensity projection image after alignment using Zeiss (AxioVision 4.0) software. Nerve fibers were traced manually using neuron reconstruction software (Neurolucida; MBF Bioscience, Williston, VT). For time course studies, corresponding points on the images from different time points were selected to make a contour, and nerve tracing was performed within the contour area. Data analysis software (NeuroExplorer; Nex Technologies, Littleton, MA) was used to measure the total length of fibers and the area of the contour in which nerves had been traced. Corneal NFD was calculated by dividing the total length of nerve fibers (mm) by the area of the contour (mm^2), as described by Al-Aqaba et al.[9]

Hematoxylin-Eosin Staining (Calculation of Flap and Bed Area)

After the surgery, mice (n = 8) were killed. Eyes were then excised, embedded in optimal cutting temperature media (Tissue-Tek, Torrance, CA), frozen on dry ice, cryosectioned into 8-μm-thick sagittal slices, and mounted onto glass slides (R 7200; Mercedes Medical, Sarasota, FL). Sections were then stained with hematoxylin-eosin and viewed using an upright microscope (Axioscope 100; Carl Zeiss Meditec GmbH). Pictures were loaded into software through a color camera. Using image archiving tools (AxioVision 4.0; Carl Zeiss Meditec GmbH), we measured the area of the flap cross-section and the underlying bed. The ratio of the flap area to the area of the whole cornea was calculated.

Corneal Whole-Mount Preparation and Confocal Microscopy

Mice were killed at 8 weeks for preparation of corneal whole mounts. Corneas were excised and directly fixed in 4% paraformaldehyde (PFA) for 1 hour. After four washes with phosphate-buffered saline (PBS, 15 minutes each), corneas were mounted onto glass slides, coated with a drop of propidium iodide-containing mounting medium, and covered with a coverslip. All steps were performed at room temperature. To study the topography of corneal nerves, we acquired confocal Z-stack images of corneal whole-mounts and performed 3D reconstruction using a confocal microscope (LSM 510 META; Carl Zeiss Meditec GmbH).

Corneal Whole-Mount Immunostaining

Nine mice were followed up for 8 weeks and then killed for immunostaining. Corneas were excised, fixed directly in 4% PFA for 1 hour at room temperature, and washed four times with PBS (for 15 minutes each). The epithelium and endothelium were removed using a blunt surgical blade to increase penetration of the reagents. Corneas were then permeabilized and blocked for 1 hour at room temperature in 1% Triton X-100, 1% bovine serum albumin (BSA), and 10% normal donkey serum in PBS. The corneas were incubated in primary antibody diluted in the blocking solution (1:100) for 72 hours at 4°C, washed four times in PBS (for 15 minutes each), and incubated with secondary antibody diluted in the blocking solution (1:350) overnight at 4°C. Corneas were further washed and mounted in mounting medium on glass slides. Primary antibodies were sheep polyclonal anti-calcitonin gene-related peptide (CGRP; catalog CA1137; Enzo Life Sciences, Plymouth Meeting, PA), rat monoclonal anti-Substance P (SP; catalog 556312; BD PharMingen, San Diego, CA), and rabbit monoclonal [EP673Y] anti-200 kDa Neurofilament Heavy (NF-200; catalog Ab40796; Abcam, Cambridge, MA). Secondary antibodies were donkey anti-sheep, anti-rat, and anti-rabbit IgG (Dylight 594-conjugated AffiniPure; Jackson ImmunoResearch, West Grove, PA). These labeled antibodies (Dylight 594) were chosen to ensure nonoverlap with the yellow fluorescent protein (YFP) wavelength and to minimize-false positive staining.

Statistical Analysis

Statistical analyses were performed using data analysis software (Excel 2003; Microsoft, Redmond, WA). One-way analysis of variance was used to compare mean values among groups. Data are expressed as the

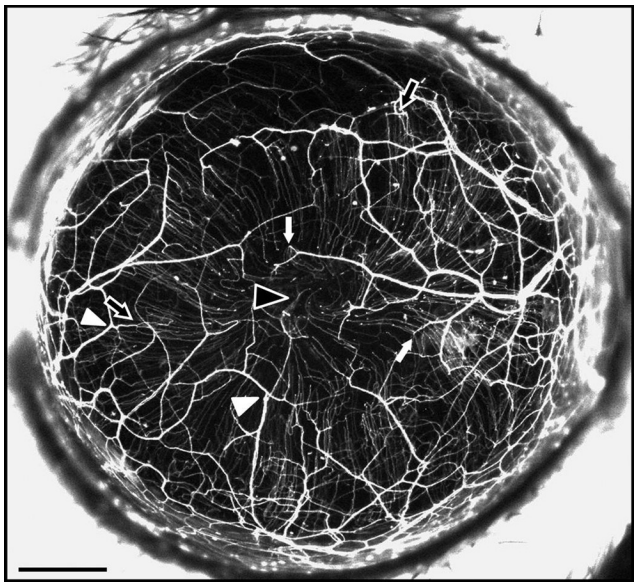

Figure 1. In vivo maximum intensity projection image of fluorescent nerves in the normal *thy1*-YFP mouse cornea. A stromal network was formed by thick nerve trunks that ran across the cornea, branching frequently (*arrowheads*) and anastomosing with adjacent nerve trunks. A second network was formed by thinner subbasal hairpin-like nerves that projected centripetally and ran roughly parallel to one another. The subbasal nerves arose from the stromal nerve trunks at variable distances from the periphery (*black arrows* indicate more peripheral origins and *white arrows* more central origins) and terminated as free endings. In some corneas, the subbasal nerves showed swirling at the corneal apex (*black arrowhead*). Intraepithelial nerves were not resolved with the stereo fluorescence microscope at the magnification used. Scale bar, 500 μm.

mean ± SE of mean. Differences were considered significant when P was < 0.05.

Results

Distribution of Nerves in the Normal Cornea

The NFD of the murine cornea was 35.3 ± 1.8 mm/mm^2. NFD was similar in all quadrants (superior, 34.5 ± 1.7 mm/mm^2; inferior, 34.6 ± 2.1 mm/mm^2; temporal, 35.2 ± 2.3 mm/mm^2; nasal, 37.0 ± 2.0 mm/mm^2; $P = 0.82$). Stromal trunks entered the cornea at the limbus, then branched frequently and anastomosed with branches from other stromal trunks. The nerve trunks ran obliquely as well as across the cornea. Along the course of these stromal trunks, thinner subbasal hairpin-like nerve offshoots arose (Fig. 1, black and white arrows). These roughly parallel hairpin nerves coursed centripetally and terminated in free nerve endings. In some corneas, the hairpin nerves showed swirling at the corneal apex (Fig. 1, black arrowhead). These hairpin nerves formed a spine from which tortuous corkscrew-like nerves arose to traverse the epithelium. These fine corkscrew epithelial nerves were visible with the confocal fluorescent microscope but not the widefield stereo fluorescent microscope.

To determine whether the distribution of corneal nerves changed over the course of this study, we performed repeated nerve imaging of murine corneas ($n = 3$) over 4 months (Fig. 2). The NFD did not significantly change (baseline, 35.3 ± 1.8 mm/mm^2; 4 weeks, 32.2 ± 2.6 mm/mm^2; 8 weeks, 37.3 ± 3.5 mm/mm^2; $P = 0.60$). The stromal nerve trunk pattern was also unchanged on serial observations (Figs. 2D–G). However, serial observations of subbasal hairpin nerves revealed the appearance of new hairpin nerves and the shortening or disappearance of other nerves (Figs. 2D–G).

Stereo Fluorescence Imaging of Nerve Regeneration after Surgery

Histologic examination ($n = 8$) showed that the average flap (epithelium + anterior stroma) area was 71.3% ± 3.5% of the total cornea (Fig. 3). After opening the tarsorrhaphies on day 3, we did not detect corneal subbasal and intrastromal nerve fluorescence within the flap area. The epithelial defect at the flap edge was healed on day 3. Stereo fluorescent imaging revealed that, at 2 weeks after surgery, sprouting of regenerating nerves was present at the transected proximal end of the stromal nerve trunks. Collateral sprouting (from uninjured nerves) was not seen from the stromal trunks. NFD was significantly reduced at 2 weeks ($P = 0.002$; 19.8 ± 1.0 mm/mm^2) and 4 weeks ($P = 0.04$; 25.63 ± 5.6 mm/mm^2) after surgery compared with the value before surgery (32.78 ± 6.1 mm/mm^2). NFD gradually increased postoperatively to 34.5 ± 2.4 mm/mm^2 at 6 weeks, with no increases in NFD seen thereafter (Fig. 4). The increase from 4 to 6 weeks (45.4% ± 3.7%) was larger than that from 2 to 4 weeks (28.8% ± 6.9%). The regenerated nerves formed a tightly interlaced network. Subbasal hairpin-like nerves were not seen in the central flap area. Collateral extensions of subbasal hairpin nerves from outside the flap toward the flap periphery were seen at week 6 onward.

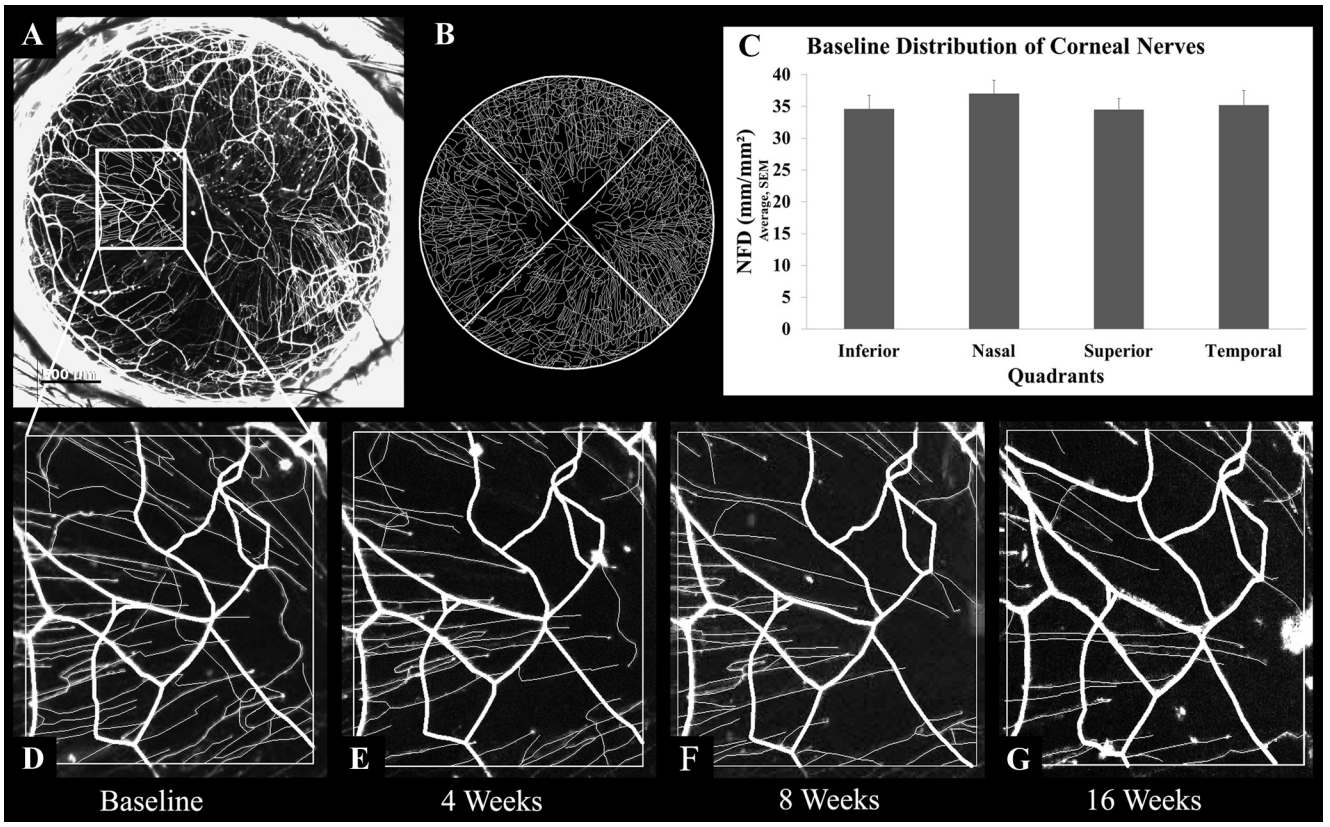

Figure 2. Nerves in normal *thy1*-YFP murine corneas. (**A**) Maximum intensity projection image of fluorescent nerves in a normal cornea. (**B**) Image generated after performing nerve tracing with neuron reconstruction software on the cornea shown in **A**. (**C**) Mean nerve fiber density in the inferior, nasal, superior, and temporal quadrants of normal corneas ($n = 3$). (**D–G**) An area of the cornea (**A**) was monitored for 0 (**D**, baseline), 4 (**E**), 8 (**F**), and 16 (**G**) weeks. Note that the subbasal hairpin nerve pattern, but not the stromal trunk pattern, changed over these serial observations. Scale bar, 500 μm.

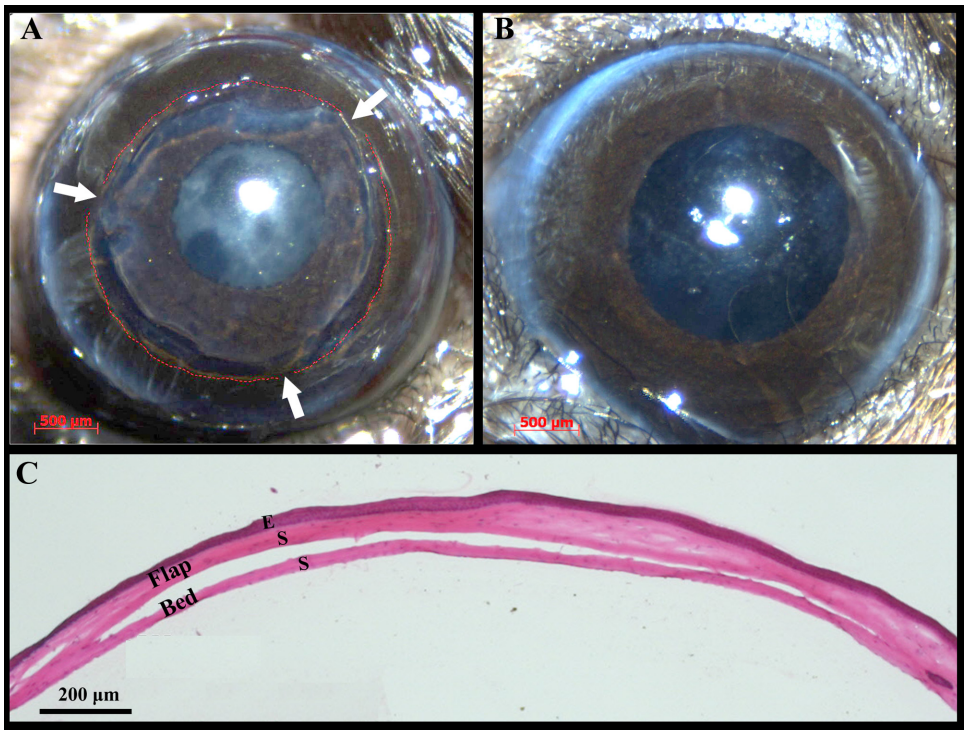

FIGURE 3. Lamellar dissection surgery in the murine cornea to transect nerves. (**A**) Cornea immediately after the lamellar dissection surgery. *Red dashed lines*: perimeter of the dissection area; *arrows*: flap hinges. Some retraction of the flap edge is evident. (**B**) The same cornea 2 weeks after surgery. No signs of scar formation, inflammation, or neovascularization are present. (**C**) Hematoxylin and eosin staining of a sagittal corneal section immediately after lamellar dissection surgery. Viscoelastic was injected in the flap-bed interface to facilitate flap area measurements. E, epithelium; S, stroma.

Whole-Mount Confocal Microscopic Analysis of Nerve Regeneration after Surgery

Whole-mount confocal microscopy was performed to compare nerve arrangement between normal corneas and postsurgical corneas. In the normal cornea, the nerves were arranged in two distinct layers (Fig. 5). However, after lamellar surgery, corneal nerves formed a dense interlaced network in the bed. The flap stroma contained nerves traversing from this network toward the epithelium. These nerves eventually terminated intraepithelially. The arrangement of corneal nerves after surgery was conspicuously missing the subbasal hairpin-like nerves in the flap center. By carefully removing the flap overlaying the bed, we were able to confirm that the interlaced network of regenerated nerves was located in the bed (Fig. 6). Finally, to determine the type of regenerating fibers, we performed whole-mount immunostaining for NF-200 (myelinated nonnociceptive fibers) and for CGRP and SP (peptidergic nociceptive fibers). In normal corneas, myelinated nerve fibers (NF200 positive) are present in the peripheral corneal stroma, whereas peptidergic nociceptive fibers (CGRP and SP positive) are present in peripheral and central stroma. We detected staining for each marker in the regenerating nerves, showing that both types of fibers were present in regenerating areas of the central stroma (Fig. 7). Whereas the presence of peptidergic nociceptive fibers in the central corneal stroma is normal, the presence of myelinated nonnociceptive fibers in the central stroma is abnormal.

DISCUSSION

This study yielded four key findings. First, transection of axons in the cornea causes regenerative sprouting from the proximal stump of stromal trunks. Notably, there was no evidence of collateral sprouting from uninjured stromal trunks. Second, NFD distal to the nerve transection gradually increases, peaking at 6 weeks with only minimal changes afterward. Third, regenerated axons do not recapitulate the normal arrangement of corneal nerves. A dense interlaced network of regenerated nerves formed in the stroma of the bed parallel to the plane of the corneal surface. Moreover, numerous fine nerves ascended from this regenerated nerve layer toward the epithelium. Fourth, large myelinated nonnociceptive nerve fibers and small unmyelinated nociceptive nerve fibers are present in regenerating fronds. We also found that, in contrast to stromal trunks, subbasal hairpin-like nerves showed changes in pattern over time, even without any intervention. This study provides a foundation for studying corneal nerve regeneration in murine models in a way not previously possible. This technique and these data can be directly applied to future investigations of molecular regulators of corneal nerve regeneration.

Our data showing absent or abnormal subbasal nerve regeneration after corneal nerve transection is similar to nerve abnormalities reported after penetrating keratoplasty (PK) and LASIK in humans.[10] In PK, all nerves passing from the periphery to the center of the cornea are transected. The corneal neuroanatomic architecture remains abnormal for months after PK.[11] Using in vivo confocal microscopy, Niederer et al.[5] have reported significant reduction in subbasal nerve fiber density and nerve branching after PK. The changes in the subbasal nerve fiber layer are apparent up to 40 years after PK. Similarly, Patel et al.[12] have reported that subbasal nerve fiber bundles were not detected in 48% of clear grafts, but when regeneration was evident, nerve fiber bundles were often tortuous and disordered. In LASIK surgery, the subbasal nerve fibers are significantly reduced in the central cornea and do not recover to near preoperative densities until 5 years after surgery.[13]

The time course of nerve regeneration in the cornea is similar to that reported by Taylor et al.[14] for changes in innervation in the lower lip after nerve lesioning. They found that NFD was significantly reduced 1 week after nerve injury and fiber density peaked at 6 weeks. Our findings differ, however, in other aspects in that we did not observe significant hyperinnervation at week 6. The changes in subbasal hairpin nerve fibers we observed could represent either dynamic changes that occur in the cornea during the constant epithelial renewal or changes with aging.[15,16] These changes might also have

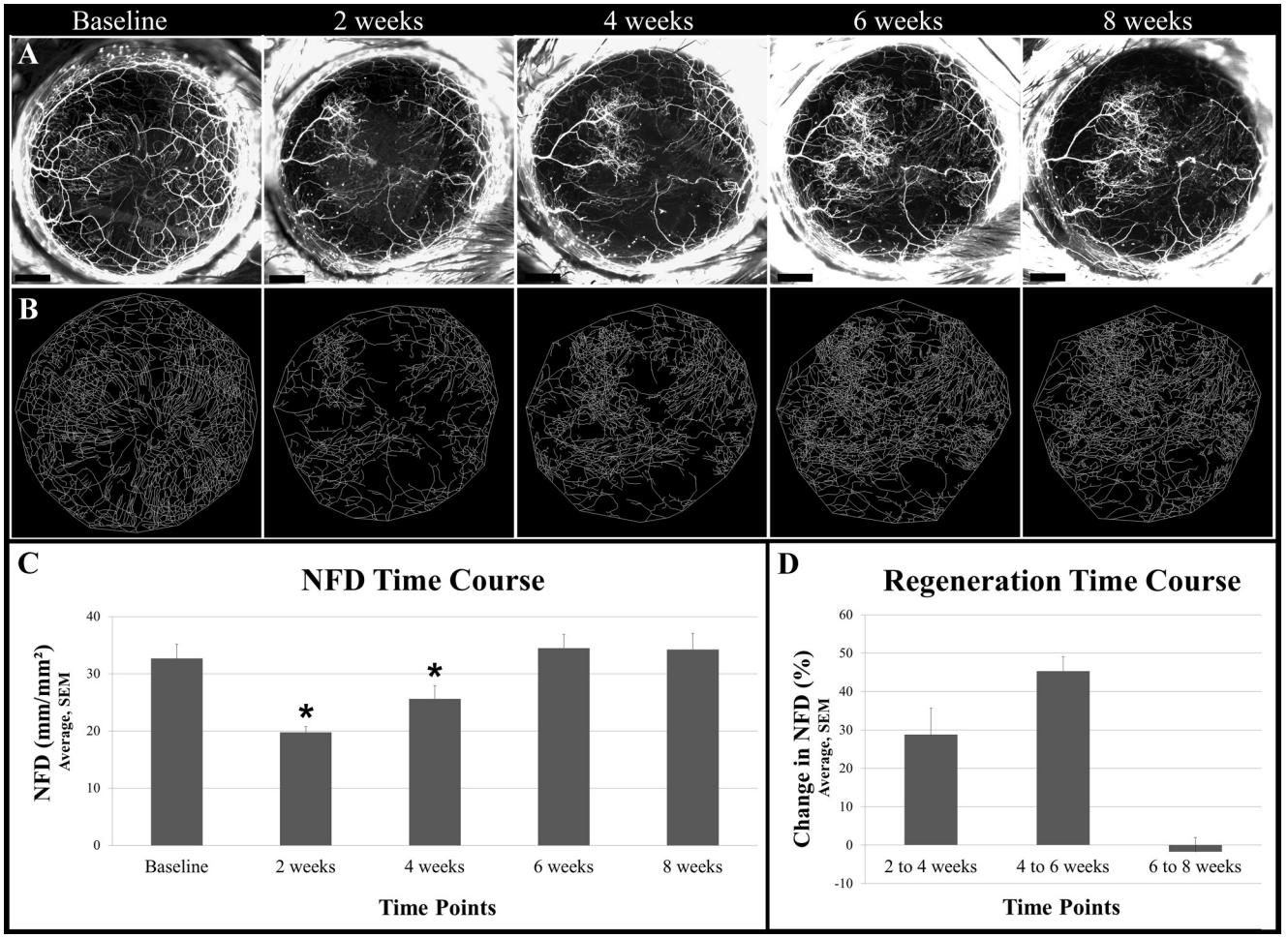

Figure 4. In vivo serial imaging of regenerating nerves after lamellar corneal surgery. (**A**) Maximum intensity projections images of the cornea showing fluorescent nerves preoperatively (baseline) and postoperatively at weeks 2, 4, 6, and 8. (**B**) Images generated after performing nerve tracing with neuron reconstruction software on the cornea shown in **A** at corresponding time points. (**C**) Mean NFD at baseline and at weeks 2, 4, 6, and 8. NFD at 2 and 4 weeks is significantly reduced compared with baseline ($P < 0.05$) (**D**) Percentage changes in NFD over weeks 2 to 4, 4 to 6, and 6 to 8. Scale bars, 500 μm.

been induced by phototoxicity to blue light, which is used to excite YFP. The cornea does not normally absorb light in the visible spectrum. However, because of the presence of YFP in the corneal nerves, there is absorption in the blue wavelength and perhaps some nerve damage because of phototoxicity. We have designed our stereo fluorescent microscope imaging protocol so that corneal light exposure is minimal. Nevertheless, any investigation of corneal nerve regeneration using our methodology should account for possible phototoxicity.

The normal cornea has extensive and complex peptidergic innervation (CGRP- and SP-positive nerves).[17] It also has a few myelinated afferents at its periphery. The main difference between the peripheral and the central stromal innervation is the presence of myelinated nerve fibers in the large peripheral stromal trunks.[18] Neurofilament 200 kDa (NF200), also known as neurofilament heavy (NF-H), is a well-established specific marker for all myelinated neurons (Aα and Aβ).[19,20] Antibodies raised against NF200 have been used to label myelinated primary afferent sensory nerve fibers in the bone periosteum,[21] skin,[22] dental pulp,[23] dorsal root ganglion,[24] and trigeminal neurons.[25] We have used antibodies specific to NF200/NF-H to determine the presence of myelinated nerve fibers in the cornea. Our data show that the regenerating fibers include peptidergic fibers as well as myelinated afferents. The presence of myelinated afferents in the central corneal stroma is abnormal. The functional significance of myelinated afferents in the central cornea during reinnervation is unknown. Further investigations will determine whether these fibers contribute to neuropathic pain after surgical transection of corneal nerves, as occurs in LASIK.[26] Although we were successful in identifying these nerve fibers in the regenerating fronds, we were unable to determine whether the distribution or proportion of these fibers differed between surgically altered and normal corneas. This limitation was largely due to inherent difficulties in immunofluorescent staining of corneal nerves in whole mounts. Improvements in whole-mount immunostaining have been proposed that may give a better outcome.[27] Peleshok et al.[22] have shown that, during nerve regeneration in the skin, after initial loss there is subsequent hyperinnervation by peptidergic nociceptive afferents but a dramatic and permanent loss of myelinated afferents. Our data show that, in contrast to regenerating skin nerves, regenerating corneal nerves contain myelinated afferents.

Transgenic mice that express fluorescent proteins in neurons under the control of regulatory elements derived from the murine *thy1* gene have been used for studying peripheral nerve degeneration and regeneration.[28,29] Greer et al.[30] used *thy1*-YFP mice to demonstrate that axotomized neurons undergo atrophy without evidence of cell death. The disappearance of YFP fluorescence in axotomized neurons signified

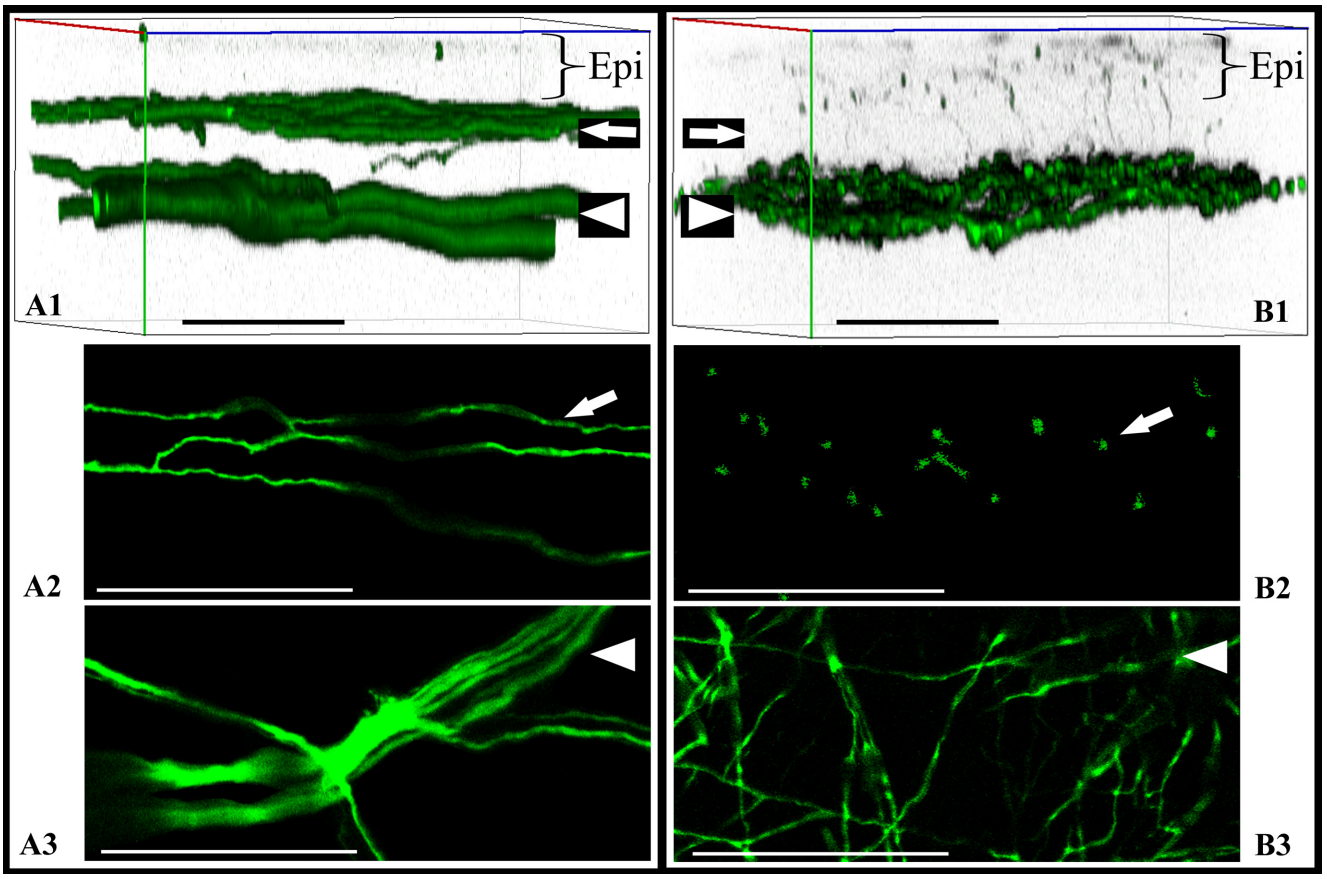

FIGURE 5. Confocal microscopy of whole-mount corneas from *thy1*-YFP mice. Images show fluorescent nerves in normal corneas (**A1–A3**) and corneas at 8 weeks after lamellar transection (**B1–B3**). Imaging was performed in the center (apex) in three separate corneas per group. Three-dimensional reconstruction of normal corneal nerves (**A1**) and regenerated corneal nerves (**B1**) showed differences in the arrangement of subbasal nerves (*arrow*) and pattern of stromal trunks (*arrowhead*). Subbasal hairpin-like nerves were seen in normal corneas (*arrow*) but not in corneas after nerve regeneration. The subbasal nerves appeared hairpin-like in normal corneas (**A2**), whereas in corneas with nerve regeneration the stroma was traversed by nerves derived from the regenerated stromal network (**B2**). Confocal sectioning shows end-on appearance of these nerves in **B2**. The deep stromal trunks in normal corneas run in well-defined bundles branching frequently at acute angles (**A3**), whereas the nerves form an interlaced network in regenerated corneas (**B3**). Scale bar, 50 μm. Epi, Epithelium.

atrophy, whereas the reappearance of YFP fluorescence fibers signified regeneration.[30] At 1 to 28 days after transection, the axotomized neurons had features consistent with regeneration of the transected proximal segment. The use of *thy1*-YFP mice for studying corneal nerves was first reported by Yu et al.[8] We have built on this mouse model to develop a methodology that makes in vivo transection and sequential observations of corneal nerve regeneration feasible.

In this study, we showed that lamellar hinged flap surgery in murine corneas is feasible and reproducible. Lamellar flap surgery of the cornea yields wide-area transection of corneal nerves with minimal confounding wound healing. Full-thick-

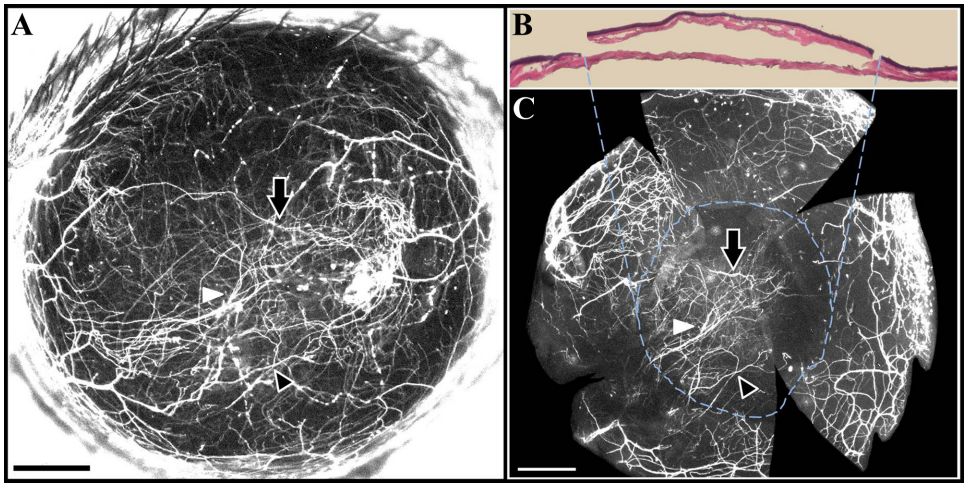

FIGURE 6. Location of regenerated nerves after lamellar surgery. (**A**) In vivo maximum intensity projection image of a cornea showing regenerated nerves at 8 weeks after surgery. (**B**) Hematoxylin and eosin staining showing excision of the flap from the cornea in **A**. (**C**) Whole-mount fluorescence image of the bed after stripping away of the flap. The regenerated stromal network was seen in the bed (*dashed circle*). *White* and *black arrowheads* and *black arrow* point to corresponding nerves in the in vivo image (**A**) and the whole-mount image (**C**) within the bed area, delineated by the *dashed circle*. Scale, 500 μm.

ness transplant surgery would have required sutures, which are known to invite inflammation and vascularization.[31] Superficial keratectomy, either surgically or with an excimer laser, would have entailed removal of the epithelium and produced subsequent epithelial migration and wound healing that would have confounded the results. Our method of corneal flap creation with four hinges obviates the need for sutures. One limitation of using flap hinges is that it cannot be determined whether a nerve trunk will traverse the hinge, thereby contributing to variability in the postoperative innervation of the flap. The use of *thy1*-YFP mice overcomes this limitation because the fluorescent corneal nerves can be visualized preoperatively, and the corneal hinge location can be determined and placed between the major nerve trunks. Our method of corneal nerve transection produces limited denervation of the cornea; therefore, we avoided epithelial and stromal disease characteristic of neurotrophic keratitis. Complete corneal denervation can be induced by trigeminal stereotactic electrolysis.[32] This procedure, when performed in mice, causes complete degeneration of subbasal and stromal corneal nerves within 48 hours. It produces corneal changes characteristic of clinical neurotrophic keratitis. The trigeminal ganglion electrolysis denervation model is suitable for investigating the mechanisms by which intact nerve function maintains normal corneal physiology, but it has limited value in investigating corneal nerve regeneration events.

The mouse strain used also affects the regeneration of nerves. The C57BL/6 mouse (strain used in this study) has been shown to regenerate axons more slowly than several other strains.[33,34] The slower regeneration rate in C57BL/6 mice might be viewed as an experimental advantage in nerve regeneration studies for two reasons. First, the slower course of regeneration increases the temporal resolution. Second, the slower rate of regeneration may make the results of effective

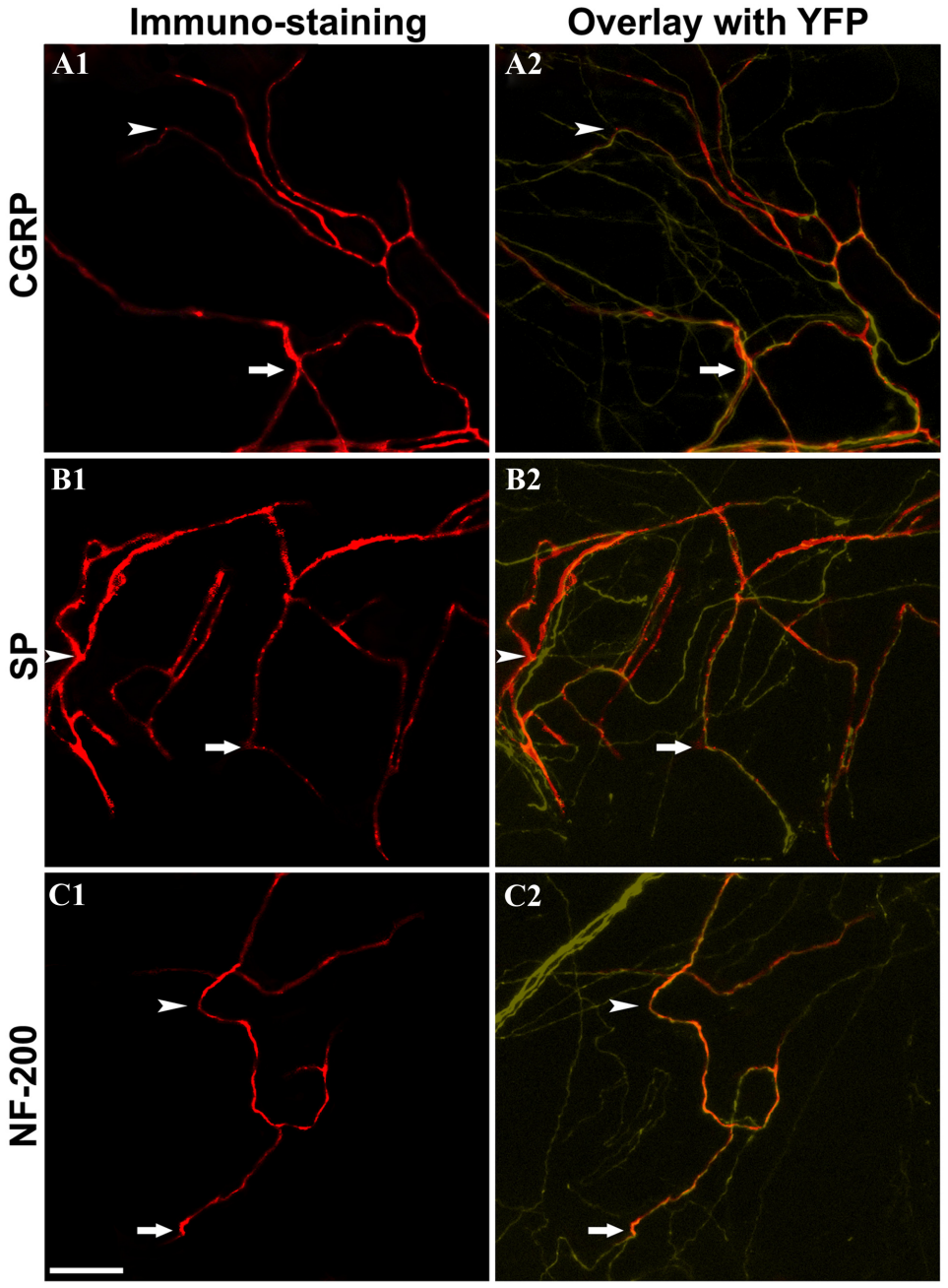

Figure 7. Whole-mount immunostaining of regenerating fibers. Corneas were stained for CGRP (**A1**, **A2**), SP (**B1**, **B2**), and NF-200 (**C1**, **C2**). Overlying YFP-positive fibers are shown in **A2**, **B2**, and **C2**. *Arrowhead* and *arrow* point to immunostained nerves (*left*) and corresponding *thy1*-YFP positive nerves (*right*). Note that regenerating fibers were positive for CGRP and SP (nociceptive nerve fibers) and for NF-200 (nonnociceptive myelinated nerve fibers). Scale bar, 50 μm.

interventions more dramatic than faster rates.[35] The use of a murine model to investigate corneal nerves has advantages because it allows for the use of well-characterized molecular tools as well as transgenic and knockout mutants. It also has disadvantages. The mice corneas are thin (approximately 100 μm centrally). Therefore, the surgical techniques tend to be more complex and to demand greater skill. Another challenge of using murine corneas is the small quantity of tissue available for gene expression or protein abundance.

We have used widefield stereo fluorescent microscopy to image the corneal nerves. At the magnification that includes the whole cornea in one field, the subbasal hairpin nerves and stromal nerve trunks, but not the intraepithelial nerves, can be resolved. We were not able to deconvolute these images for 3D reconstruction because, in stereo microscopy, the images are taken off axis. Hence, we have presented the data from the in vivo images as maximum intensity projection NFD. The key to making corneal NFD observations is to control eye movements that occur with normal breathing and to constrict the pupil completely to mask the retinal fluorescence. We used a gas mask to stabilize the head and control movements associated with breathing. We constricted pupils with carbachol 0.01%, which causes complete constriction within approximately 5 minutes and lasts for approximately 20 minutes. We initially used pilocarpine 1% to 2%; however, we found that it produces incomplete pupillary constriction and a high incidence of respiratory distress and death (unpublished data, 2010).

In conclusion, we performed lamellar surgery in the cornea to transect the nerves and then monitored the reinnervation by in vivo fluorescent imaging. Our results suggest that regenerating nerves do not completely readopt the normal arrangement of fibers in the cornea.

Acknowledgments

The authors thank Bryn Namavari for help with image processing.

References

1. Bonini S, Rama P, Olzi D, Lambiase A. Neurotrophic keratitis. *Eye.* 2003;17:989–995.
2. Dastjerdi MH, Dana R. Corneal nerve alterations in dry eye-associated ocular surface disease. *Int Ophthalmol Clin.* 2009;49:11–20.
3. Wilson SE. Laser in situ keratomileusis-induced (presumed) neurotrophic epitheliopathy. *Ophthalmology.* 2001;108:1082–1087.
4. Moilanen JA, Holopainen JM, Vesaluoma MH, Tervo TM. Corneal recovery after LASIK for high myopia: a 2-year prospective confocal microscopic study. *Br J Ophthalmol.* 2008;92:1397–1402.
5. Niederer RL, Perumal D, Sherwin T, McGhee CN. Corneal innervation and cellular changes after corneal transplantation: an in vivo confocal microscopy study. *Invest Ophthalmol Vis Sci.* 2007;48:621–626.
6. Patel SV, Erie JC, McLaren JW, Bourne WM. Keratocyte and subbasal nerve density after penetrating keratoplasty. *Trans Am Ophthalmol Soc.* 2007;105:180–189.
7. He J, Bazan HE. Omega-3 fatty acids in dry eye and corneal nerve regeneration after refractive surgery. *Prostaglandins Leukot Essent Fatty Acids.* 2010;82:319–325.
8. Yu CQ, Rosenblatt MI. Transgenic corneal neurofluorescence in mice: a new model for in vivo investigation of nerve structure and regeneration. *Invest Ophthalmol Vis Sci.* 2007;48:1535–1542.
9. Al-Aqaba MA, Alomar T, Miri A, Fares U, Otri AM, Dua HS. Ex vivo confocal microscopy of human corneal nerves. *Br J Ophthalmol.* 2010;94:1251–1257.
10. Darwish T, Brahma A, Efron N, O'Donnell C. Subbasal nerve regeneration after penetrating keratoplasty. *Cornea.* 2007;26:935–940.
11. Stachs O, Zhivov A, Kraak R, Hovakimyan M, Wree A, Guthoff R. Structural-functional correlations of corneal innervation after LASIK and penetrating keratoplasty. *J Refract Surg.* 2010;26:159–167.
12. Patel SV, Erie JC, McLaren JW, Bourne WM. Keratocyte density and recovery of subbasal nerves after penetrating keratoplasty and in late endothelial failure. *Arch Ophthalmol.* 2007;125:1693–1698.
13. Erie JC, McLaren JW, Hodge DO, Bourne WM. Recovery of corneal subbasal nerve density after PRK and LASIK. *Am J Ophthalmol.* 2005;140:1059–1064.
14. Taylor AM, Ribeiro-da-Silva A. GDNF levels in the lower lip skin in a rat model of trigeminal neuropathic pain: Implications for nonpeptidergic fiber reinnervation and parasympathetic sprouting. *Pain.* 2011;152:1502–1510.
15. Hanna C, Bicknell DS, O'Brien JE. Cell turnover in the adult human eye, *Arch Ophthalmol.* 1961;65:695–698.
16. Harris LW, Purves D. Rapid remodeling of sensory endings in the corneas of living mice. *J Neurosci.* 1989;9:2210–2214.
17. Jones MA, Marfurt CF. Peptidergic innervation of the rat cornea. *Exp Eye Res.* 1998;66:421–435.
18. Müller LJ, Pels L, Vrensen GF. Ultrastructural organization of human corneal nerves. *Invest Ophthalmol Vis Sci.* 1996;37:476–488.
19. Ruscheweyh R, Forsthuber L, Schoffnegger D, Sandkühler J. Modification of classical neurochemical markers in identified primary afferent neurons with Abeta-, Adelta-, and C-fibers after chronic constriction injury in mice. *J Comp Neurol.* 2007.10;502:325–336.
20. Lever IJ, Robinson M, Cibelli M, et al. Localization of the endocannabinoid-degrading enzyme fatty acid amide hydrolase in rat dorsal root ganglion cells and its regulation after peripheral nerve injury. *J Neurosci.* 2009;29:3766–3780.
21. Castañeda-Corral G, Jimenez-Andrade JM, Bloom AP, et al. The majority of myelinated and unmyelinated sensory nerve fibers that innervate bone express the tropomyosin receptor kinase A. *Neuroscience.* 2011;178:196–207.
22. Peleshok JC, Ribeiro-da-Silva A. Delayed reinnervation by nonpeptidergic nociceptive afferents of the glabrous skin of the rat hindpaw in a neuropathic pain model. *J Comp Neurol.* 2011;519:49–63.
23. Paik SK, Lee DS, Kim JY, et al. Quantitative ultrastructural analysis of the neurofilament 200-positive axons in the rat dental pulp. *J Endod.* 2010;36:1638–1642.
24. Ho C, O'Leary ME. Single-cell analysis of sodium channel expression in dorsal root ganglion neurons. *Mol Cell Neurosci.* 2011;46:159–166.
25. Staikopoulos V, Sessle BJ, Furness JB, Jennings EA. Localization of P2X2 and P2X3 receptors in rat trigeminal ganglion neurons. *Neuroscience.* 2007;144:208–216.
26. Nettune GR, Pflugfelder SC. Post-LASIK tear dysfunction and dysesthesia. *Ocul Surf.* 2010;8:135–145.
27. Liu H, Kao WW. A novel protocol of whole mount electro-immunofluorescence staining. *Mol Vis.* 2009;15:505–517.
28. Unezaki S, Yoshii S, Mabuchi T, Saito A, Ito S. Effects of neurotrophic factors on nerve regeneration monitored by in vivo imaging in thy1-YFP transgenic mice. *J Neurosci Methods.* 2009;178:308–315.
29. Yan Y, Sun HH, Mackinnon SE, Johnson PJ. Evaluation of peripheral nerve regeneration via in vivo serial transcutaneous imaging using transgenic Thy1-YFP mice. *Exp Neurol.* 2011 Jul 1 [Epub ahead of print].
30. Greer JE, McGinn MJ, Povlishock JT. Diffuse traumatic axonal injury in the mouse induces atrophy, c-Jun activation, and axonal outgrowth in the axotomized neuronal population. *J Neurosci.* 2011;31:5089–5105.
31. Cursiefen C, Maruyama K, Jackson DG, Streilein JW, Kruse FE. Time course of angiogenesis and lymphangiogenesis after brief corneal inflammation. *Cornea.* 2006;25:443–447.
32. Ferrari G, Chauhan SK, Ueno H, et al. A novel mouse model for neurotrophic keratopathy: trigeminal nerve stereotactic electrolysis through the brain. *Invest Ophthalmol Vis Sci.* 2011;52:2532–2539.
33. Xin L, Richardson PM, Gervais F, Skamene E. A deficiency of axonal regeneration in C57Bl/6J mice. *Brain Res.* 1990;510:144–146.
34. Xin L, Skamene E, Richardson PM. Studies of axonal regeneration in C57BL/6J and A/J mice. *Brain Res.* 1994;652:174–176.
35. Griffin JW, Pan B, Polley MA, Hoffman PN, Farah MH. Measuring nerve regeneration in the mouse. *Exp Neurol.* 2010;223:60–71.